5

Frequency-Domain Analysis of Linear Control Systems

5.1 STEADY-STATE RESPONSES TO SINUSOIDAL INPUTS

While the impulse and step functions are useful test signals to use in the characterization of linear systems, it is difficult to find naturally occurring signals that approximate these highly idealized waveforms. Moreover, abrupt steps and impulsive changes are difficult to generate as test signals. On the other hand, periodic phenomena are a common occurrence in physiology. Since it is possible, using the *Fourier series*, to decompose any periodic signal into its sinusoidal components, sine waves represent a highly useful class of basic test inputs. Furthermore, sinusoidal changes are generally much easier to approximate in practice relative to other periodic and most nonperiodic signals.

5.1.1 Open-Loop Frequency Response

Consider the linearized respiratory mechanics model (open-loop case) discussed in the previous chapter, expressed in differential equation form (see Figure 4.2a):

$$LC\frac{d^2P_A}{dt^2} + RC\frac{dP_A}{dt} + P_A = P_{ao} \tag{5.1}$$

Suppose the input P_{ao} were to assume the form of a sinusoidal waveform of amplitude X_0 and angular frequency ω. Note that ω is related to absolute frequency, f, by the following relationship:

$$\omega = 2\pi f \tag{5.2}$$

To simplify the mathematics, we employ the generalized sinusoidal (or complex exponential) function instead of the sine or cosine:

$$P_{ao}(t) = X_0 e^{j\omega t} \tag{5.3}$$

where X_0 is a real constant. Solution of the inhomogenous differential equation, Equation (5.1), in which the right-hand side takes the particular form shown in Equation (5.3), yields a solution for P_A that contains two parts, as discussed previously in Section 2.5. The complementary function represents the transient part of the response, while the particular solution characterizes the steady-state response. In this discussion, we will be concerned only with the steady-state response in P_A. With the input given by Equation (5.3), the only way for equality to hold for arbitrary values of t (time) between the left-hand and right-hand sides of Equation (5.1) is for the particular solution of P_A to contain the function $e^{j\omega t}$. Thus, we assume the following form for $P_A(t)$:

$$P_A(t) = Ze^{j\omega t} \tag{5.4}$$

which states that the output of the system defined by Equation (5.1) must also be sinusoidal with the same frequency as the input signal. In Equation (5.4), we allow the function Z to be complex. Substituting Equation (5.4) into Equation (5.1), we obtain, after canceling $e^{j\omega t}$ from both sides of the equation and rearranging terms:

$$Z = H_o(\omega)X_0 \tag{5.5}$$

where

$$H_o(\omega) = \frac{1}{(1 - LC\omega^2) + jRC\omega} \tag{5.6}$$

$H_o(\omega)$ is a complex function of the frequency of the input and can be expressed in polar form as

$$H_o(\omega) = |H_o(\omega)|e^{j\phi_o(\omega)} \tag{5.7}$$

where the magnitude is

$$|H_o(\omega)| = \frac{1}{\sqrt{(1 - LC\omega^2)^2 + R^2C^2\omega^2}} \tag{5.8}$$

and the phase component is

$$\phi_o(\omega) = -\tan^{-1}\left(\frac{RC\omega}{1 - LC\omega^2}\right) \tag{5.9}$$

The complex function $H_o(\omega)$ represents the relationship between the sinusoidal input $P_{ao}(t)$ and the sinusoidal output $P_A(t)$. Substituting Equation (5.5) and (5.7) back into Equation (5.4), we obtain the following expression for $P_A(t)$:

$$P_A(t) = |H_o(\omega)|X_0e^{j(\omega t + \phi(\omega))} \tag{5.10}$$

Since $P_{ao}(t)$ is $X_0e^{j\omega t}$, Equation (5.10) imples that, although the output $P_A(t)$ remains sinusoidal at the same angular frequency ω, its amplitude and phase are different from those of $P_{ao}(t)$. The ratio between the output and input amplitudes, or the *gain*, is given by $|H_o(\omega)|$, while the *phase difference* is represented by $\phi_o(\omega)$. It is important to note that both gain and phase difference are functions of the forcing frequency ω. Figure 5.1 shows predictions of $P_A(t)$ produced by the lung mechanics model when $P_{ao}(t)$ assumed the form of sinusoidal waves of *unit amplitude* at absolute frequencies of 1, 4, and 8 Hz. The values of the parameters employed here were $R = 0.3\,\text{cm}\,H_2O\,s\,L^{-1}$, $C = 0.1\,L\,\text{cm}\,H_2O^{-1}$, and $L = 0.01\,\text{cm}\,H_2O\,s^2\,L^{-1}$. At very low frequencies, P_A oscillates virtually in synchrony with

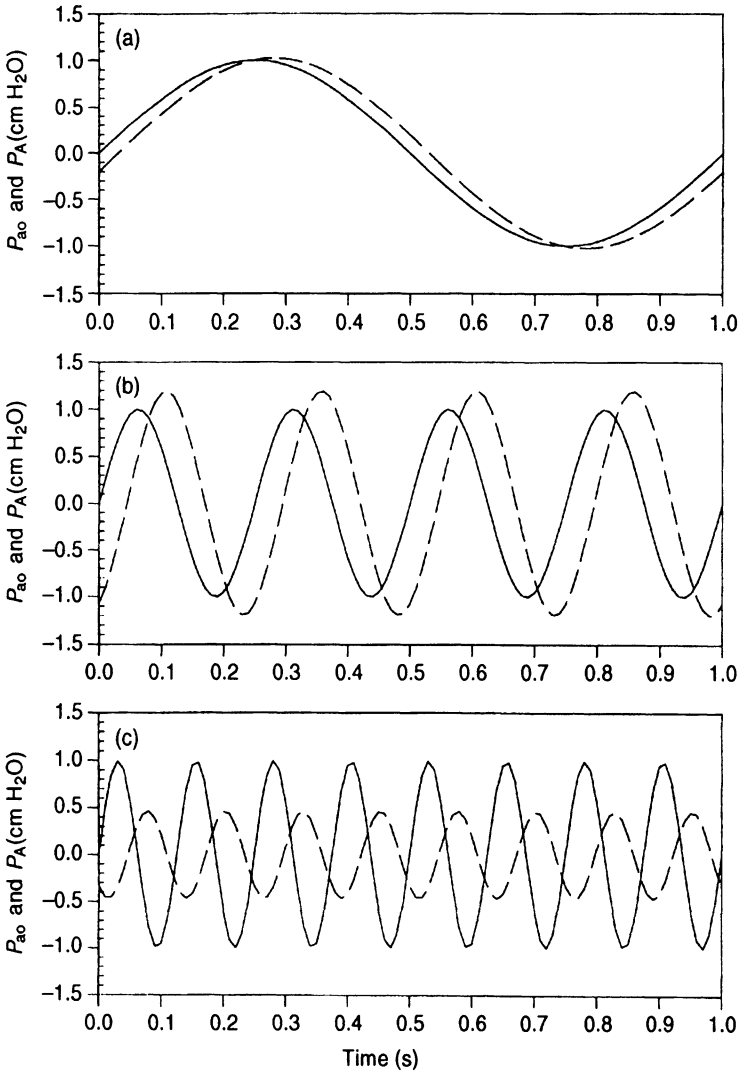

Figure 5.1 Steady-state responses (dashed tracings) at P_A of linearized lung mechanics model to sinusoidal excitation (solid tracings) at P_{ao}. Frequencies of sine waves are (a) 1 Hz, (b) 3 Hz and (c) 8 Hz.

P_{ao} and is of the same amplitude. At very high frequencies, P_A lags substantially behind P_{ao} and is significantly attenuated. Using this set of parameters, however, there is a range of frequencies over which P_A is amplified and becomes larger in amplitude than P_{ao}. The amplification is greatest at approximately 4 Hz. If one determined the impulse or step response for this model with these parameter values, one would find an underdamped response with an oscillation frequency of about 4 Hz. Thus, exciting the system with an external sinusoidal input at this frequency produces *resonance*, since the applied forcing acts to reinforce the natural vibrations of the system.

The complex function $H_o(\omega)$ contains all the information shown in Figure 5.1 and much more. It predicts how the lung mechanics model will respond to sinusoidal inputs of unit amplitude and all possible frequency values. As such, it is also called the *frequency response* of the system. Figure 5.2 illustrates one method of graphically representing the

frequency response of the lung mechanics model. At each absolute frequency, f, we evaluate the gain and phase of $H_o(\omega)$. Two frequency responses are shown in this diagram. The first represents the underdamped system, with $R = 0.3\,\text{cm}\,H_2O\,s\,L^{-1}$; this frequency response encompasses the results shown in Figure 5.1. The second frequency response shown represents the overdamped system where $R = 1\,\text{cm}\,H_2O\,s\,L^{-1}$. In this case, it is clear that there is no resonance peak, so that the gain continually decreases with increasing frequency.

Note from Equation (4.4) that the transfer function corresponding to the lung mechanics model described by Equation (5.1) is

$$H_o(s) \equiv \frac{P_A(s)}{P_{ao}(s)} = \frac{1}{LCs^2 + RCs + 1} \tag{5.11}$$

An alternative approach to deriving the frequency response function $H_o(\omega)$ is by evaluating $H_o(s)$ along the imaginary axis on the s-plane, i.e., *by setting* $s = j\omega$. Substituting $j\omega$ for s in Equation (5.11), we obtain

$$H_o(\omega) = \frac{1}{LC(j\omega)^2 + RCj\omega + 1} \tag{5.12}$$

Since $j^2 = -1$, rearranging terms in Equation (5.12) leads to Equation (5.6).

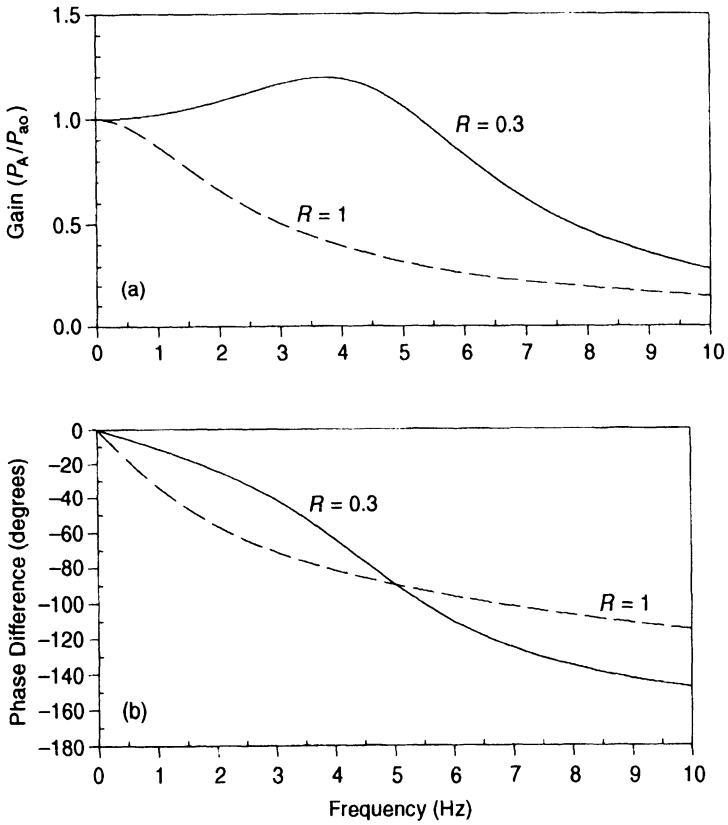

Figure 5.2 Frequency responses of the linearized lung mechanics model in underdamped (solid curves) and overdamped (dashed curves) conditions. The values shown for R are in cm $H_2O\,s\,L^{-1}$. Other parameter values are $C = 0.1$ L cm H_2O^{-1} and $L = 0.01$ cm $H_2O\ s^2\ L^{-1}$.

5.1.2 Closed-Loop Frequency Response

Now, consider the closed-loop situation where there is proportional feedback of $P_A(t)$. The corresponding transfer function would be as given in Equation (4.5b). Evaluating the frequency response, we obtain

$$H_c(\omega) = \frac{1}{(1 + k - LC\omega^2) + jRC\omega} \tag{5.13}$$

Thus, for the closed-loop case, the magnitude and phase of the frequency response are given by

$$|H_c(\omega)| = \frac{1}{\sqrt{(1 + k - LC\omega^2)^2 + R^2C^2\omega^2}} \tag{5.14}$$

and

$$\phi_c(\omega) = -\tan^{-1}\left(\frac{RC\omega}{1 + k - LC\omega^2}\right) \tag{5.15}$$

The closed-loop frequency responses are shown together with the open-loop responses in Figure 5.3. Here, the feedback gain k has been assumed to be unity. Closing the loop leads to a reduction of the steady-state gain from 1 to 0.5, i.e., $|H_c(\omega = 0)| = 0.5$ compared to $|H_o(\omega = 0)| = 1$. This is consistent with the results that were previously presented in Chapters 3 and 4. Closing the loop also shifts the location of the resonance peak to a substantially higher frequency (~6.5 Hz) versus ~4 Hz). This also is consistent with the impulse and step responses of the underdamped system in Chapter 4 where we found an increase in frequency but decrease in amplitude of the transient oscillations. The phase portion of the frequency response shows a general decrease in the phase lag introduced by the closed-loop system vis-à-vis the open-loop system. This is equivalent to our earlier finding in Chapter 4 that closing the loop produces an increase in the speed of response of the system.

5.1.3 Relationship between Transient and Frequency Responses

Since the transfer function of any linear system is the Laplace transform of its impulse response and the frequency response can be deduced by replacing s in the Laplace transform by $j\omega$, it follows that the frequency response can be derived by taking the Fourier transform of the impulse response. This implies that one should be able to deduce various features of the transient response from the corresponding frequency response. Consider an idealized linear system with the following frequency response:

$$\begin{aligned} H(\omega) &= e^{-j\omega\tau}, & -\omega_c \le \omega \le \omega_c \\ &= 0, & |\omega| > \omega_c \end{aligned} \tag{5.16}$$

i.e., this system has a gain of unity at angular frequencies between $-\omega_c$ and ω_c and zero gain at all frequencies outside this range. The *bandwidth* of a linear system is defined as the range of frequencies over which the system gain exceeds $1/\sqrt{2}$ or 0.7071 (see sections to follow). Thus, in this case, ω_c represents the system bandwidth. The phase of this system is linear with

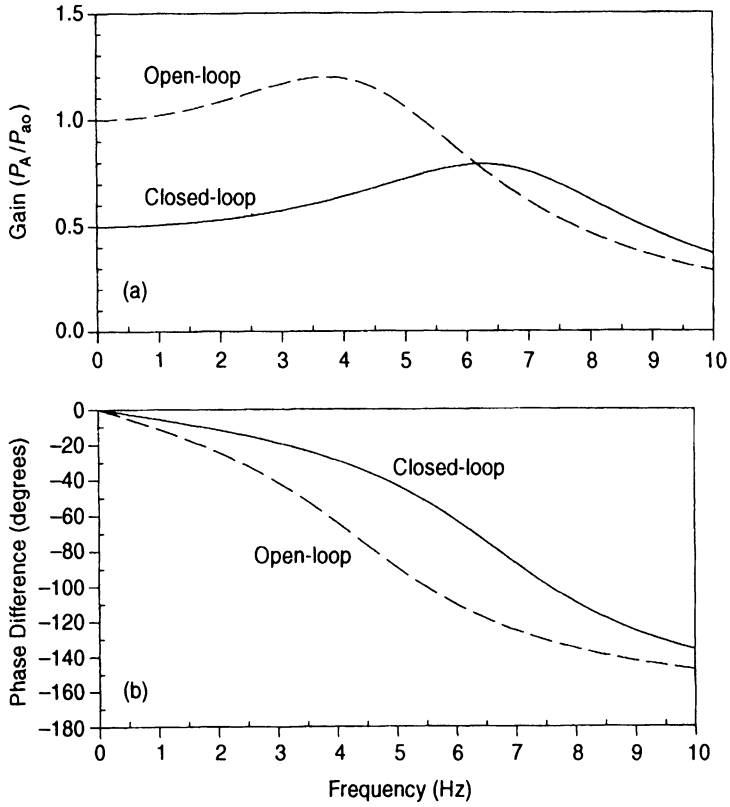

Figure 5.3 Frequency responses of the linearized lung mechanics model in closed-loop (solid curves) and open-loop modes. The values of the parameters used are: $R = 0.3$ cm H_2O L^{-1}, $C = 0.1$ L cm H_2O^{-1}, $L = 0.01$ cm H_2O s^2 L^{-1}, and $k = 1$ (or equivalently, $\lambda = 2$).

frequency within the bandwidth; the slope of the phase curve (line) is $-\tau$, i.e., the output is delayed by τ relative to the input at all frequencies. This frequency response is displayed in Figures 5.4a and 5.4b.

To deduce the corresponding impulse response, $h(t)$, we take the inverse Fourier transform of Equation (5.16):

$$\begin{aligned} h(t) &= \frac{1}{2\pi}\int_{-\infty}^{\infty} H(\omega)e^{j\omega t}\,d\omega \\ &= \frac{1}{2\pi}\int_{-\omega_c}^{\omega_c} e^{-j\omega\tau}e^{j\omega t}\,d\omega \\ &= \frac{\omega_c}{\pi}\text{sinc}[\omega_c(t-\tau)] \end{aligned} \tag{5.17}$$

where the function sinc(x) represents $\sin(x)/x$. Figure 5.4c shows the form of $h(t)$. Note three important features in Equation (5.17). First, the impulse response peaks τ units of time after the input impulse has occurred, due to the delay inherent in $H(\omega)$. Secondly, the maximum value of the impulse response or the *peak amplitude* (see Section 4.4.2.1) is proportional to the bandwidth ω_c. This makes sense since a larger bandwidth allows the impulse response to

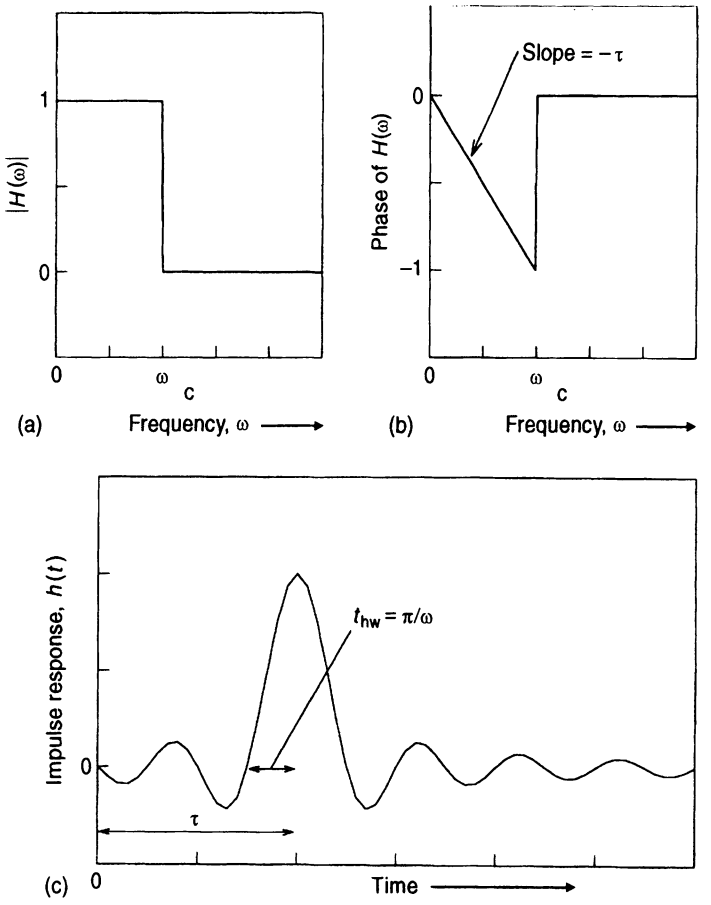

Figure 5.4 Relationship between frequency response (a and b) and the impulse response (c) of a linear system.

be composed of a broader range of frequencies: in particular, the higher frequencies add sharpness or abruptness to the impulse response. In the limit, as bandwidth becomes infinite, the peak amplitude also becomes infinite as the impulse response approaches a delta function, i.e., the same form as the input itself. The third important feature relates to the *half-width*, t_{hw}, of the impulse response, i.e., the time taken for the main response to the impulse to fully develop. From Equation (5.17), t_{hw} can be deduced from the interval between the impulse response peak and the preceding or subsequent zero-crossing (see Figure 5.4c):

$$t_{hw} = \frac{\tau}{\omega_c} \tag{5.18}$$

Since the step response is simply the integral of the impulse response, it also can be shown that the rise time, T_r, of the step response is proportional to t_{hw} and therefore inversely proportional to ω_c. In fact, for a second-order system such as our linearized lung mechanics model, the following approximate relationship holds:

$$T_r \approx \frac{2}{\omega_c} \tag{5.19}$$

As we discussed in Section 4.4.1, the *natural frequency* ω_n and *damping ratio* ζ are the two key parameters that characterize the impulse and step responses of the generalized second-order linear system. These parameters can easily be derived from the frequency response of the same system. Consider the linearized lung mechanics model in open-loop mode, the frequency response of which is given by Equations (5.8) and (5.9). Note from Equation (4.49) in Section 4.4.1 that $\omega_n = 1/(LC)^{1/2}$. Thus, $1 - LC\omega_n^2 = 0$, so that $\phi_o(\omega_n) = -\tan^{-1}(\infty) = -90°$. Therefore, by locating the frequency at which the phase plot attains a phase lag of 90°, we can deduce ω_n. Evaluation of the frequency response magnitude at ω_n allows us to deduce ζ, since

$$|H_o(\omega_n)| = \frac{1}{RC\omega_n} = R\sqrt{\frac{C}{L}} = \frac{1}{2\zeta} \tag{5.20}$$

where the last equality in Equation (5.20) is based on Equation (4.50) in Section 4.4.1.

For the (open-loop) case where $L = 0.01$, $C = 0.1$, and $R = 0.3$, note that $\omega_n = 31.62\,\text{rad s}^{-1}$, corresponding to a frequency of approximately 5 Hz. At this frequency, $|H_o(\omega_n)| \sim 1.05$. It is important to note that this does not correspond to the *resonant frequency*, which is located at ~4 Hz ($\omega_r \sim 25$). Moreover, the peak value of $|H_o(\omega)|$, which occurs at the resonant frequency, is ~1.2. In fact, resonance occurs at the natural frequency only when there is no damping in the system ($R = 0$).

5.2 GRAPHICAL REPRESENTATIONS OF FREQUENCY RESPONSE

5.2.1 Bode Plot Representation

In the field of control engineering, Bode plots represent one of the most accepted classical methods for displaying the frequency response of a linear system. These plots are similar to but differ from the graphs presented in Figures 5.2 and 5.3 in that the gain (or magnitude) and frequency scales are presented in logarithmic form, while the phase remains on a linear scale. In addition, the frequency scale is generally displayed in terms of the angular frequency, ω, and therefore in units of radians per second.

The gain of the frequency response, $H(\omega)$, is expressed in units of *decibels* (dB), defined as follows:

$$\begin{aligned} G_{\text{dB}}(\omega) &= 10\ \log_{10}|H(\omega)|^2 \\ &= 20\ \log_{10}|H(\omega)| \end{aligned} \tag{5.21}$$

The first equality in Equation (5.21) is shown to emphasize the fact that for a linear system, $|H(\omega)|^2$ represents the ratio between the *power* of the output and the power of the input signal. The value of ω at which only half of the input signal power is transmitted is known as the *corner* or *cut-off* frequency, ω_c. Thus, $|H(\omega_c)|^2 = 0.5$. Since $|H(\omega_c)| = 1/\sqrt{2}$, it turns out that the range of frequencies between 0 and ω_c is also the system bandwidth, as discussed previously. Using Equation (5.21), we find that $G_{\text{dB}}(\omega_c) = -3\,\text{dB}$. This definition assumes only the case where the system takes the form of a low-pass filter, where the high frequencies are attenuated. For systems that are high-pass in nature, the corner frequency is defined as the frequency at which the input signal power is amplified and doubled at the output. In this case, $|H(\omega_c)|^2 = 2$, and therefore, $G_{\text{dB}}(\omega_c) = 3\,\text{dB}$. Thus, in general, the corner frequency is the frequency at which the gain of the linear system is changed by 3 dB.

The logarithmic nature of G_{dB} represents one of the major strengths of the Bode plot. In general, it is possible to factorize the numerator and denominator of any given frequency response function into a cascade of first-order systems. For instance, consider the following generalized frequency response function:

$$H(\omega) = \frac{G_{SS} \prod_{m=1}^{M} (1 + j\omega\tau_m)}{(j\omega)^N \prod_{i=1}^{P} (1 + j\omega\tau_i)} \tag{5.22}$$

Note that in Equation (5.22), G_{SS} is the steady state gain for the case $N = 0$. If we express the magnitude of $H(\omega)$ in terms of logarithmic gain, then

$$G_{dB}(\omega) = 20 \log_{10} \left[\frac{G_{SS} \prod_{m=1}^{M} \sqrt{1 + \omega^2\tau_m^2}}{\omega^N \prod_{i=1}^{P} \sqrt{1 + \omega^2\tau_i^2}} \right] \tag{5.23a}$$

Evaluating the logarithm of the expression in brackets in Equation (5.23a), we obtain

$$G_{dB}(\omega) = 20 \log_{10} G_{SS} + \sum_{m=1}^{M} 20 \log_{10}(1 + \omega^2\tau_m^2)^{1/2} + 20 \log_{10} \omega^{-N} + \sum_{i=1}^{P} 20 \log_{10}(1 + \omega^2\tau_i^2)^{-1/2} \tag{5.23b}$$

This representation converts the logarithm of the products of several factors into equivalent sums of the logarithms of these factors. As a result, the contribution of each term is additive, which makes it easy to determine how the individual factors contribute to the overall gain. The overall phase of $H(\omega)$ can also be decomposed into the sum of all its individual components:

$$\phi(\omega) = \sum_{m=1}^{M} \tan^{-1}(\omega\tau_m) - \frac{N\pi}{2} - \sum_{i=1}^{P} \tan^{-1}(\omega\tau_i) \tag{5.24}$$

From the above example, one can see that it is useful to consider the magnitude and phase contributions of the basic components of $H(\omega)$, which take the form of either $(j\omega)^{-1}$ or $(1 + j\omega\tau)^{\pm 1}$. Let us first consider the term $(j\omega)^{-1}$. Note that since $j\omega$ is purely imaginary and has no real part, its phase contribution is $\pi/2$ radians. Consequently, the phase contribution of $(j\omega)^{-N}$ is $-N\pi/2$ radians, the negative sign implying that the phase shift is a lag. The magnitude contribution of $(j\omega)^{-N}$ is infinite at zero frequency but zero at infinite frequency.

Now, consider the term $(1 + j\omega\tau)$. This factor adds a phase shift of $+\tan^{-1}(\omega\tau)$, i.e., a phase lead, to $H(\omega)$. At very low frequencies ($\omega \ll 1/\tau$), this phase lead would be close to zero. At very high frequencies, i.e., $\omega \gg 1/\tau$, this phase lead would approach $\pi/2$ radians or 90°. What about the gain contributions of this factor? At very low frequencies ($\omega \ll 1/\tau$), the gain would be $\sim 20 \log_{10}(1) = 0$ dB, i.e., this would appear as a straight line on the zero-decibel axis. At very high frequencies ($\omega \gg 1/\tau$), the gain would approximate $20 \log_{10}(\omega\tau)$ dB, and thus behave like a straight line (on the Bode plot) with a slope of 20 dB/decade. These two straight lines bound the actual gain plot and are known as the *low-frequency* and *high-frequency asymptotes*, respectively. Conversely, each $(1 + j\omega\tau)^{-1}$ factor would contribute a phase shift of $-\tan^{-1}(\omega\tau)$, i.e., a phase lag, to $H(\omega)$. As in the previous

case, at very low frequencies the phase lag would approach zero while the low-frequency asymptote for the gain plot would coincide with the zero-decibel axis. At very high frequencies, the phase lag would approach 90°, and the high-frequency asymptote for the gain plot would be a straight line with slope −20 dB/decade. The Bode plots for these two basic functions are displayed in Figure 5.5, together with the low-frequency and high-frequency asymptotes.

The Bode plots of the frequency response of the linearized lung mechanics model discussed earlier are presented in Figure 5.6. It should be noted that these plots contain the same information as the linear frequency response plots displayed in Figure 5.3. One difference is that the frequency scale is expressed in terms of ω, in units of radians per second. Another important feature is that the logarithmic scaling enhances the appearance of the resonance peaks in both the open-loop and closed-loop systems. In both cases, the bandwidth of the system can be readily determined as the frequency range over which the gain lies above −3 dB relative to the steady-state gain level.

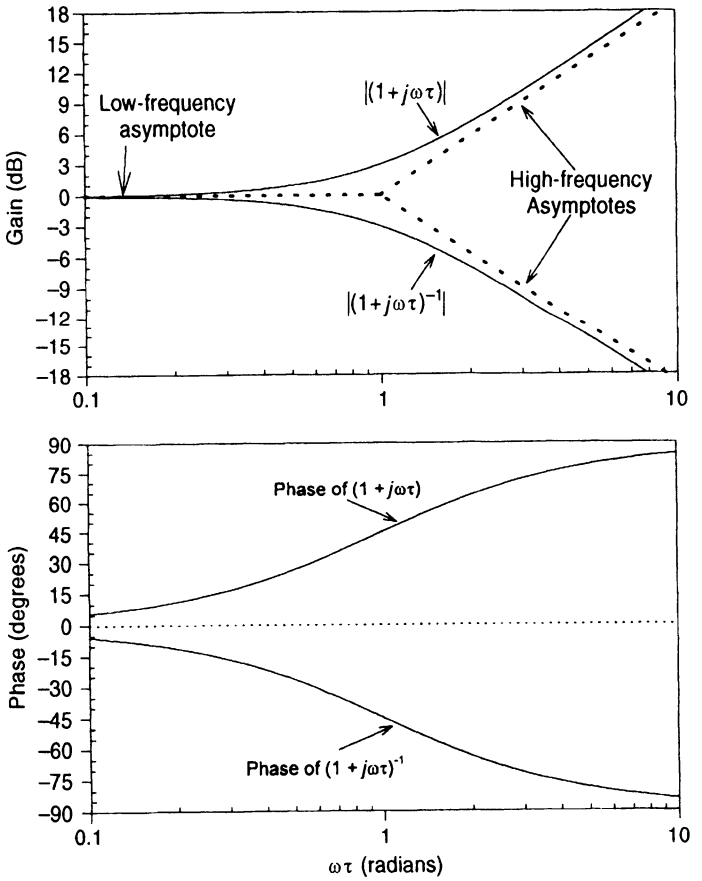

Figure 5.5 Bode plots of the first-order frequency response functions $(1 + j\omega\tau)$ and $(1 + j\omega t)^{-1}$. Note, in this case, that the "frequency scale" has been normalized and presented in terms of the product "$\omega\tau$."

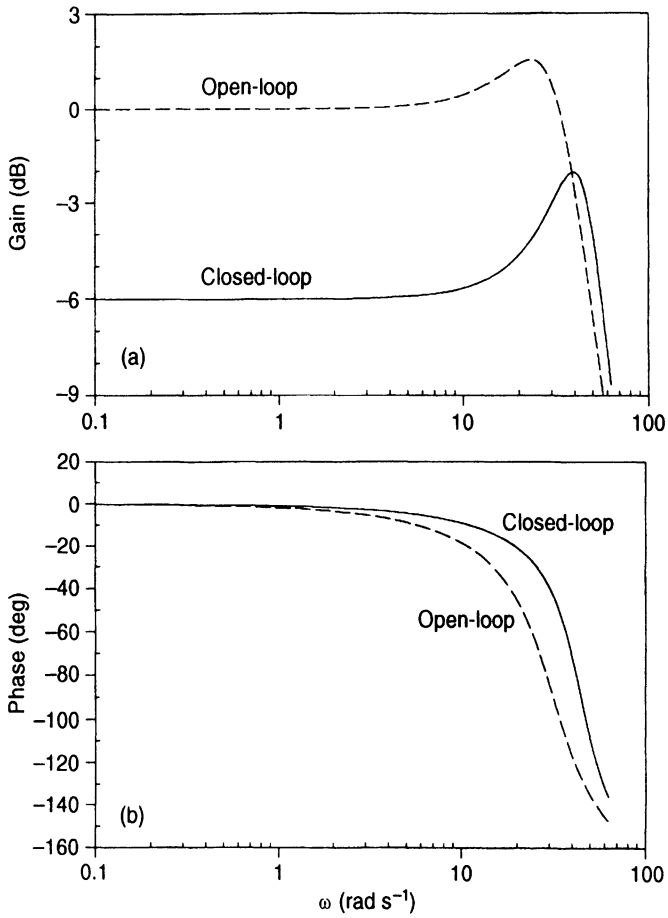

Figure 5.6 Bode plots of the frequency response of the linearized lung mechanics model in open-loop and closed-loop modes.

5.2.2 Nichols Charts

Instead of presenting gain and phase in separate plots, an alternative approach is to plot the logarithmic magnitude in dB versus phase for a range of frequencies. These plots are known as *Nichols charts*. The log-magnitude vs. phase curves for the frequency responses $(1 + j\omega\tau)$ and $(1 + j\omega\tau)^{-1}$ are displayed in Figure 5.7. The solid circles on these plots correspond to the frequencies listed. In this case, the individual values of the product $\omega\tau$ are shown, so that the same plots would apply irrespective of the specific value of τ being employed. Figure 5.8 shows the Nichols charts for the linearized lung mechanics model in open-loop and closed-loop modes. The values placed next to the closed circles represent the corresponding angular frequencies, ω, in radians per second. These curves convey the same information that was contained in the Bode plots of Figure 5.6 and the linear frequency response plots of Figure 5.3. However, as we will see later, the shapes of these curves at the points where gain approaches 0 dB and the phase approaches $-180°$ can yield useful information about system stability.

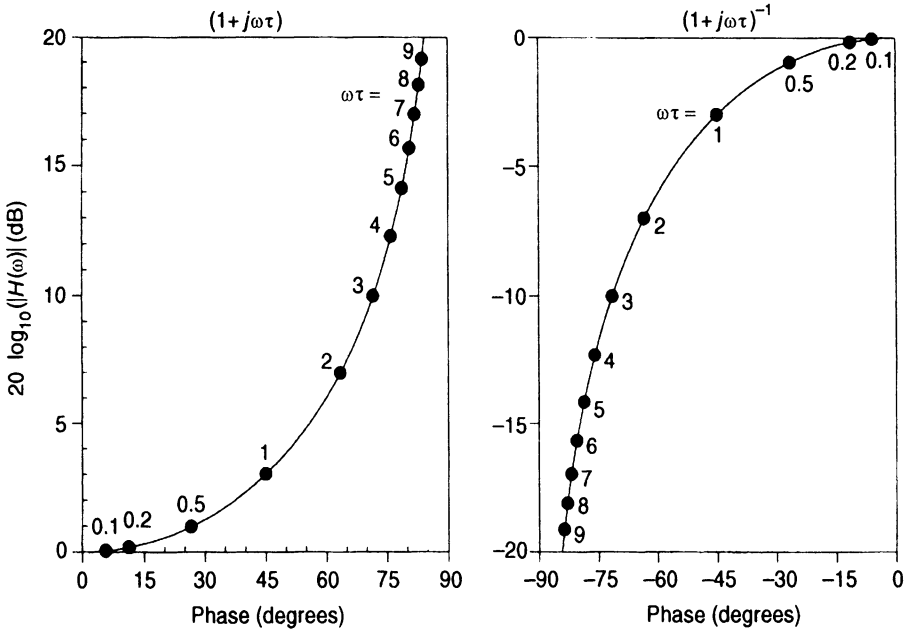

Figure 5.7 Nichols charts for the frequency response functions $(1+j\omega\tau)$ and $(1+j\omega\tau)^{-1}$.

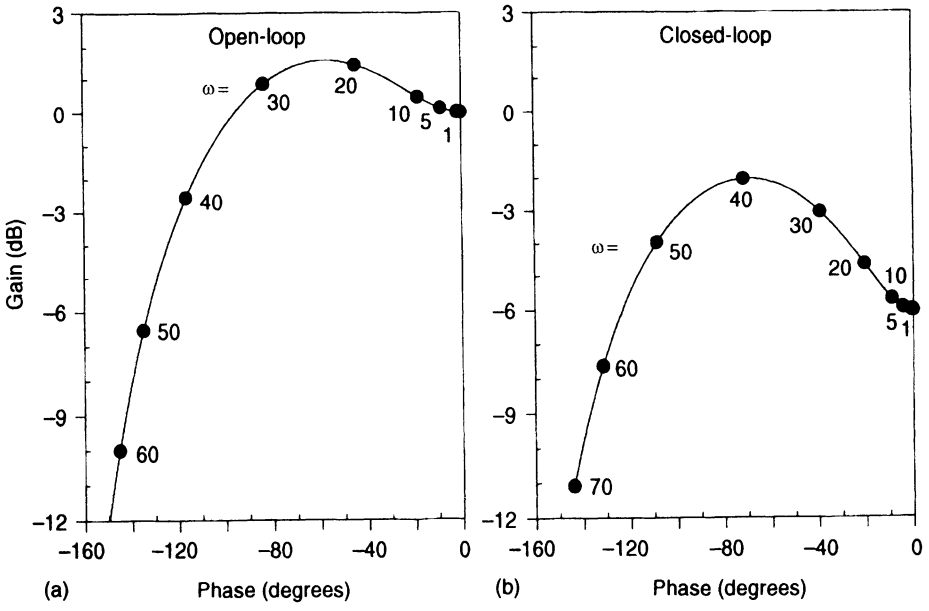

Figure 5.8 Nichols charts for the linearized lung mechanics model in open-loop (a) and closed-loop (b) modes. The parameter values assumed are the same as the values employed in Figures 5.3 and 5.5.

5.2.3 Nyquist Plots

Nyquist plots are sometimes also called *polar plots*. Here, the frequency response $H(\omega)$ is plotted on a plane in which the horizontal axis reflects the magnitude of the real part of $H(\omega)$ while the vertical axis reflects the imaginary part. Thus, at any frequency ω, $H(\omega)$ is represented by a vector linking the origin to the point in question, and the length of the vector represents the magnitude of $H(\omega)$. As illustrated in the inset in Figure 5.9, the angle subtended by this line and the positive real axis represents ϕ, the phase of $H(\omega)$. The sign convention generally adopted is that *anticlockwise* rotations of the vector $H(\omega)$ from the positive real axis yield *positive values* for ϕ.

Nyquist plots corresponding to the basic frequency response functions $1/j\omega\tau$, $(1+j\omega\tau)$ and $(1+j\omega\tau)^{-1}$ are shown in Figure 5.9. The plot for $1/j\omega\tau$ coincides with the negative portion of the imaginary axis: when $\omega = 0$, $1/j\omega\tau$ is at $-j\infty$, but as ω becomes large, $1/j\omega\tau$ approaches the origin along the imaginary axis. The locus of $(1+j\omega\tau)$ begins with a gain of unity on the real axis. As ω increases, this frequency response function moves vertically upward, tracing a path that is parallel with the positive imaginary axis. By contrast, the locus traced by $(1+j\omega\tau)^{-1}$ is a semi-circular arc that begins at 1 on the real axis when $\omega = 0$ and ends at the origin when $\omega = \infty$.

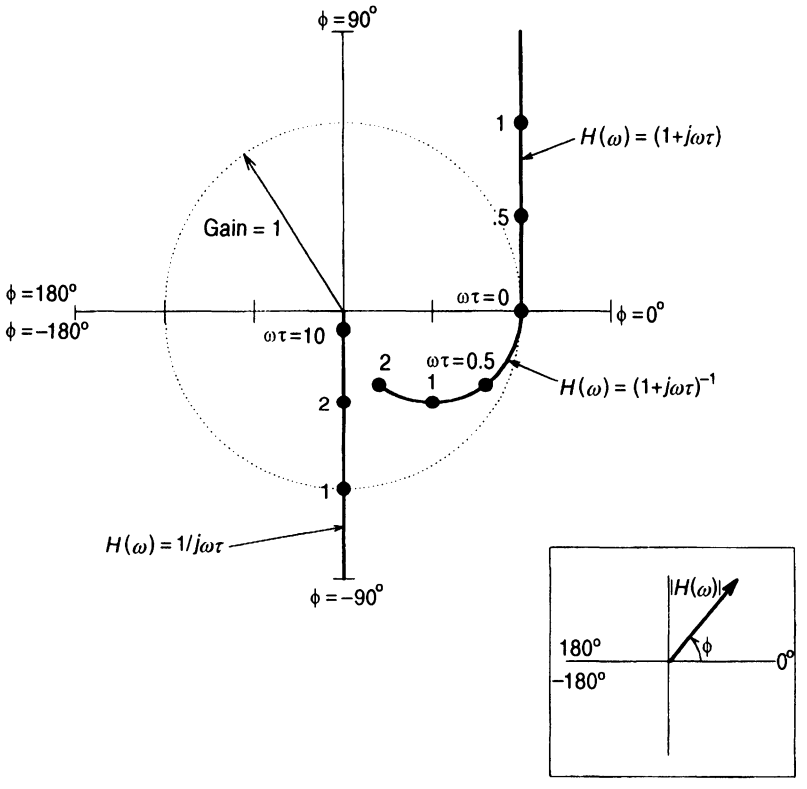

Figure 5.9 Nyquist plots for the basic frequency response functions $1/j\omega\tau$, $(1+j\omega\tau)$, and $(1+j\omega\tau)^{-1}$. Selected values of $\omega\tau$ are shown as solid circles. The dotted circle represents the locus of points where gain equals unity. Inset shows definitions of $|H(\omega)|$ and ϕ—anticlockwise rotations of vector $H(\omega)$ from the positive real axis yield positive values of ϕ, and vice versa.

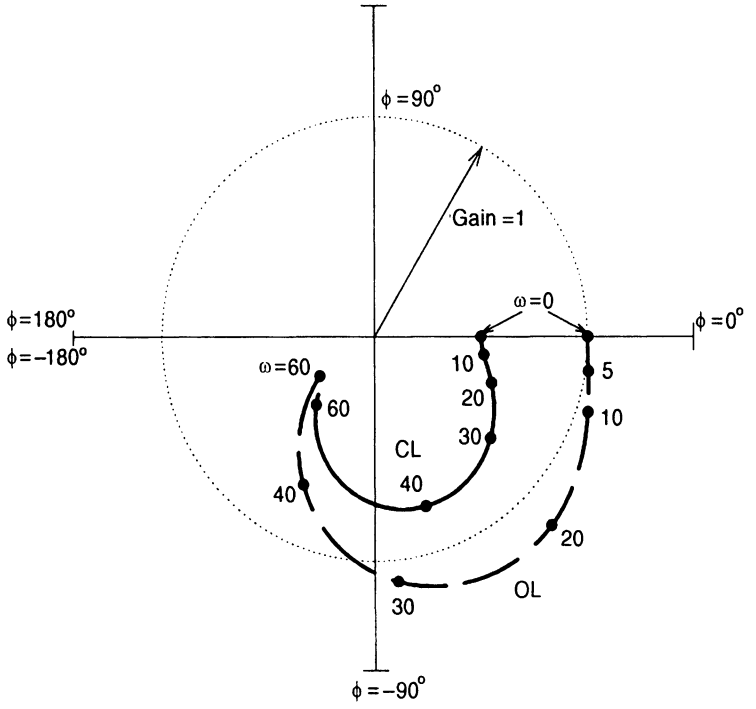

Figure 5.10 Nyquist plots for the frequency responses of the linearized lung mechanics model in open-loop (OL, broken curve) and closed-loop (CL, solid curve) modes. The dotted circle represents the locus of points at which the gain equals 1.

The loop-like forms of the Nyquist plots presented in Figure 5.10 are more representative of the frequency responses of physiological systems. The particular plots shown characterize the frequency responses of the linearized lung mechanics model in both open-loop and closed-loop modes. These frequency responses represented here are exactly the same as those shown in Figure 5.3 where magnitude and phase were separately plotted against frequency. However, it is clear from the Nyquist plots that the points at which these curves intersect the imaginary axis (i.e., when $\phi = -90°$ and $\omega = \omega_n$) do not correspond to the points of resonance at which the gain is maximum (and $\omega = \omega_r$).

5.3 FREQUENCY-DOMAIN ANALYSIS USING MATLAB AND SIMULINK

5.3.1 Using MATLAB

To demonstrate the utility of employing MATLAB to examine the frequency response of a known system, we turn again to our linearized model of lung mechanics. We will use the closed-loop transfer function expression given in Equation (4.5b), since this can be converted to the open-loop expression by simply setting k equal to zero. Assuming that the values of L, R, C, and k have been preassigned, the following command lines set up the transfer function, `Hs`, of the model and produces the frequency vector `w` which contains the range of frequencies (in rad s^{-1}) to be examined:

```
>> num = [1];
>> den = [L*C  R*C  (1 + k)];
>> Hs = tf(num, den);
>> f = 0:0.1:10
>> w = 2*pi*f;
```

The MATLAB Control System Toolbox function `freqresp` is used next to compute the frequency response, `Hw`, of `Hs` over the frequency range of 0 to 10 Hz. Since `Hw` is a complex mutlidimensional array, the `squeeze` function is used to collapse it into a complex vector, which is subsequently decomposed into magnitude and phase components using the `abs` and `angle` functions, respectively. Finally, the magnitude and phase components are plotted against `w`.

```
>> Hw = freqresp(Hs, w);
>> Hwmag = abs(squeeze(Hw))';
>> Hwpha = 180* angle (squeeze (Hw}))/pi;
>> subplot(2,1,1); plot(w,Hwmag);
>> ylabel('Freq Resp Magnitude'); grid on;
>> subplot(2,1,2); plot(w,Hwpha);
>> xlabel('Frequency (rad/s)');
>> ylabel('Freq Resp Phase (deg)'); grid on;
```

The above command lines will produce linearly-scaled frequency response plots of the type shown in Figures 5.2 and 5.3.

To produce Bode plots, the following commands can be used:

```
>> bode(Hs,w);
>> [Hwmag, Hwpha] = bode(Hs, w};
```

The first command line will lead to the automatic generation of Bode gain and phase diagrams. The second command line will not produce the plots but will save the results in the variables "`Hwmag`" and "`Hwpha`."

In similar fashion, the Nichols chart can be generated using the following lines:

```
>> nichols (Hs,w);
>> [Hwmag, Hwpha] = nichols(Hs, w);
```

Again, the second line will only compute the results but will not produce the plots.

Finally, the Nyquist plot can be produced as follows:

```
>> nyquist(Hs,w);
>> [Hwreal, Hwimag] = nyquist(Hs, w);
```

In this case, however, the second command line yields the real and imaginary parts of the frequency response, `Hw`, and not the magnitude and phase.

All of the above command lines are contained in a script file called "`fda_llm.m`," which has been included in the library of MATLAB and SIMULINK files that accompany this book.

5.3.2 Using SIMULINK

The MATLAB functions described in the previous section are extremely useful when the exact transfer function of the system being analyzed is known. However, with more complicated models where there may exist several subsystems connected through forward and feedback loops, deriving a closed form for the overall frequency response can be very laborious. In such situations, an alternative approach would be to perturb the model with a known input, monitor the resulting output, and use both input and output to deduce the frequency response of the system. This is a basic *system identification* technique; systems identification and parameter estimation will be discussed in greater detail in Chapter 7.

Figure 5.11 provides an illustration of how the frequency response of our linearized lung mechanics model can be "measured." Here, we assume the following values for the model parameters (see Equation (4.5b)): $L = 0.01\,\mathrm{cm\,H_2O\,s^2\,L^{-1}}$, $R = 0.3\,\mathrm{cm\,H_2O\,s\,L^{-1}}$, $C = 0.1\,\mathrm{L\,cm\,H_2O^{-1}}$, and $k = 1$ (i.e., closed-loop mode), so that the particular transfer function employed here is given by

$$H(s) = \frac{1}{0.001s^2 + 0.03s + 2} \tag{5.25}$$

This model is represented in Figure 5.11 by the LTI system block, labeled `Hs`, found in the SIMULINK Controls Toolbox library. Although `Hs` is represented by the simple form shown in this example, in general it could be composed of several interconnected subsystems. The point of relevance here is that one has to identify the input and output that relate to the overall transfer function of the model. White noise is fed into the input of `Hs`, and both input and output are fed into a block known as `Spectrum Analyzer`, found in the `Extra Sinks` sublibrary of the `Simulink Extras` blockset. The `Spectrum Analyzer` produces the graphical results shown in Figure 5.12, where the top panel displays the input and output time-courses, and the lower two panels show the frequency response magnitude and phase. Note that since the results displayed are computed from datasets of finite duration, it is inevitable that "noise" will appear in the estimated frequency response plots. The model

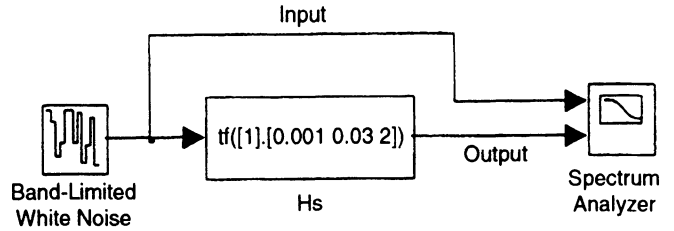

Figure 5.11 SIMULINK model used for determining the frequency response of the linearized lung mechanics (closed-loop) transfer function.

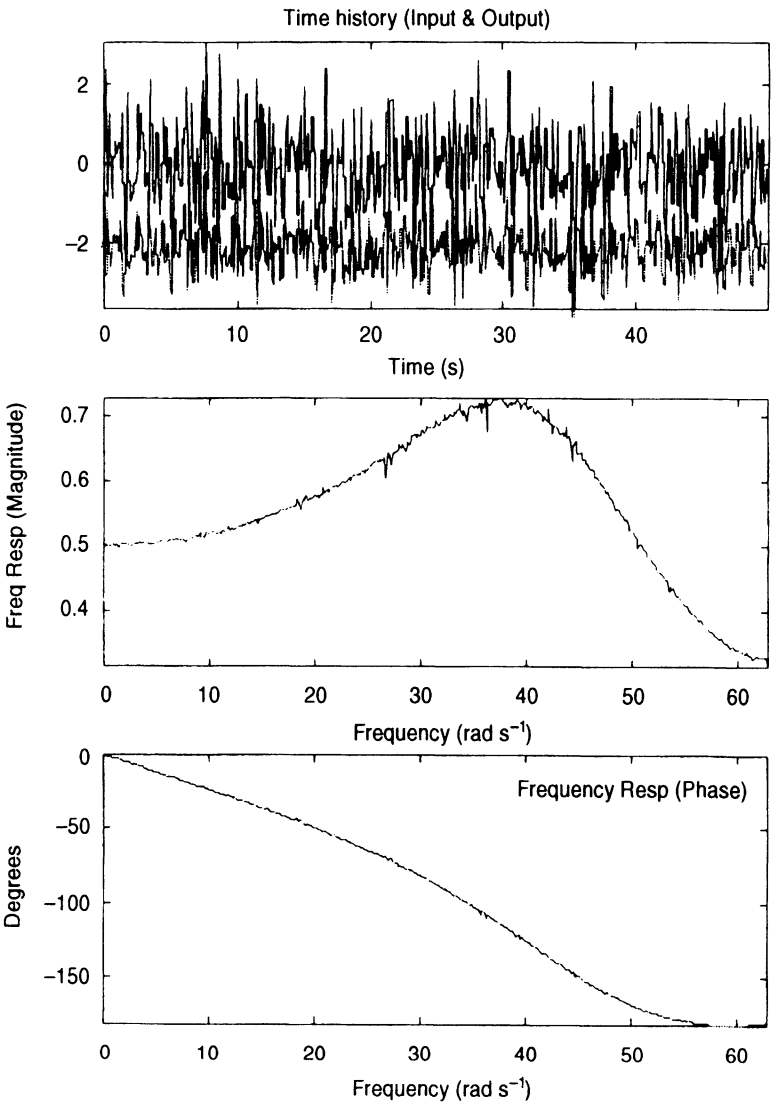

Figure 5.12 Determination of frequency response of linearized lung mechanics model using the SIMULINK program shown in Figure 5.11. Top panel shows time-courses of the input to and output from the model. Note that the actual mean level of the output signal was zero: the displayed time-course was shifted vertically to enhance clarity of presentation.

shown in Figure 5.11 has been saved in the SIMULINK model file "`fdallm2.mdl`," which may be found in the library of MATLAB/SIMULINK files that accompany this book.

The algorithm embedded in `Spectrum Analyzer` is based on the following principle that is valid for all linear systems: The frequency response of the system under study can be derived by dividing the cross-spectrum of the input and output by the spectrum of the input. This principle is derived from the basic linear properties of convolution and superposition. Assuming $x(t)$ and $y(t)$ to represent the input and output of the linear system

with impulse response $h(t)$, we begin by recalling the convolution equation displayed in Equation (2.45):

$$y(t) = \int_0^\infty h(t')x(t - t')\, dt' \tag{5.26}$$

Multiplying both sides of Equation (5.26) by $x(t - \tau)$ and then taking expectations, we obtain

$$E[x(t - \tau)y(t)] = \int_0^\infty h(t')E[x(t - \tau)x(t - t')]\, dt' \tag{5.27a}$$

where the *expectations* operator $E[\cdot]$ is defined by

$$E[z] = \int_{-\infty}^\infty zp(z)\, dz \tag{5.28}$$

and $p(z)$ is the probability distribution function of the variable z. However, by definition, the left-hand side of Equation (5.27a) yields the *cross-correlation* function between x and y, $R_{xy}(\tau)$, while the expectation term on the right-hand side is equal to the *autocorrelation* function of x, $R_{xx}(\tau)$. Thus, we replace Equation (5.27a) with

$$R_{xy}(\tau) = \int_0^\infty h(t')R_{xx}(\tau - t')\, dt' \tag{5.27b}$$

It can be shown that *Fourier transformation* of R_{xy} and R_{xx} yields the cross-spectrum S_{xy} and autospectrum S_{xx}, respectively; this equivalence principle is also known as the *Wiener–Khinchine* theorem. And since the frequency response $H(\omega)$ is obtained by Fourier transforming $h(t)$, the time-convolution on the right-hand side of Equation (5.27b) can be converted into a product in the frequency domain:

$$S_{xy}(\omega) = H(\omega)S_{xx}(\omega) \tag{5.29a}$$

where

$$S_{xy}(\omega) = \int_{-\infty}^\infty R_{xy}(\tau)e^{-j\omega\tau}\, d\tau, \tag{5.30a}$$

$$S_{xx}(\omega) = \int_{-\infty}^\infty R_{xx}(\tau)e^{-j\omega\tau}\, d\tau \tag{5.30b}$$

$$H(\omega) = \int_{-\infty}^\infty h(\tau)e^{-j\omega\tau}\, d\tau \tag{5.30c}$$

Thus, the frequency response can be estimated from

$$H(\omega) = \frac{S_{xy}(\omega)}{S_{xx}(\omega)} \tag{5.29b}$$

Note that for good estimates of $H(\omega)$ to be derived from Equation (5.29b), it is important for S_{xx} to be positive over the range of interest for ω. Ideally, the input or stimulus signal should have a spectrum that is relatively flat over a wide bandwidth, i.e., the input should be *broadband*. In fact, the optimal type of input, from the viewpoint of estimation, is white noise (see Chapter 7).

An important detail that the user should note is that, when setting up `Spectrum Analyzer`, a value is required for the "`Sampling Interval`." This value allows the block to assign a time-scale to the input and output data. The sampling interval also

determines the frequency range over which the estimated frequency response is plotted. In our example, we were concerned with the frequency range of 0 to 10 Hz, corresponding to a range in ω of 0 to $\sim 63\,\text{rad}\,\text{s}^{-1}$. Thus, we chose a minimum sampling frequency of 20 Hz, which translated to a sampling interval of 0.05 s.

5.4 FREQUENCY RESPONSE OF A MODEL OF CIRCULATORY CONTROL

The regulation of heart rate and systemic blood pressure is achieved in the short-term primarily through the feedback control via the arterial baroreflexes. However, both cardiovascular variables are continually perturbed by respiration. Breathing can affect heart rate and arterial blood pressure through a number of mechanisms. First, respiratory-induced intrathoracic pressure changes exert a direct effect on arterial pressure which, in turn, affects heart rate through the baroreflexes. Secondly, the present evidence suggests a direct coupling between the respiratory pattern generator in the medulla and the autonomic centers that influence heart rate. Thirdly, vagal feedback from the pulmonary stretch receptors during breathing has been shown to reflexively affect heart rate. And, finally, changes in heart rate can lead to changes in cardiac output which, in turn, produce arterial blood pressure fluctuations that alter heart rate through the baroreflexes. The overall effect of respiration on heart rate, commonly referred to as the *respiratory sinus arrhythmia*, can be quantified in terms of a frequency response function. Changes in phase and/or magnitude of this frequency response function would suggest changes in one of the factors that influence autonomic control of heart rate.

5.4.1 The Model

The model of circulatory control that we will examine was developed by Saul and coworkers (1991) from the Harvard Medical School and Massachusetts Institute of Technology. The SIMULINK implementation of this model (filename: "`rsa.mdl`") is shown in Figure 5.13. Respiration, measured in the form of lung volume change, V, is assumed to directly affect the autonomic inputs to the sinoatrial node: inspiration leads to decreases in both vagal and sympathetic efferent activity (note signs in summing blocks). The model does not distinguish between respiratory input from the pulmonary stretch receptors from the central drive that originates in the medullary centers. Feedback from the baroreceptors also directly influences the autonomic inputs to the heart: a rise in arterial blood pressure, `abp`, produces a decrease in sympathetic activity and an increase in parasympathetic activity. During inspiration, the decrease in vagal efferent activity acts on the sinoatrial node to increase heart rate, `hr`. The transfer function that models the dynamics of this relationship is a simple low-pass filter with a cutoff frequency (fp) that is on the order of 0.2 Hz and a negative gain, $-K_p$. In contrast, the response of the sinoatrial node to sympathetic stimulation is considerably slower. In addition to a latency of 1–2 s, the transfer function that characterizes the dynamics of sympathetic activity to heart rate conversion has a cutoff frequency, fs, of 0.015 Hz. In this case, the gain is positive.

Changes in heart rate are assumed to affect arterial blood pressure after a delay of 0.42 s. For simplicity, the transfer function representing the properties of the arterial vasculature is assumed static with a gain of $0.01\,(\text{mm Hg})\,\text{min bt}^{-1}$. As well, since the

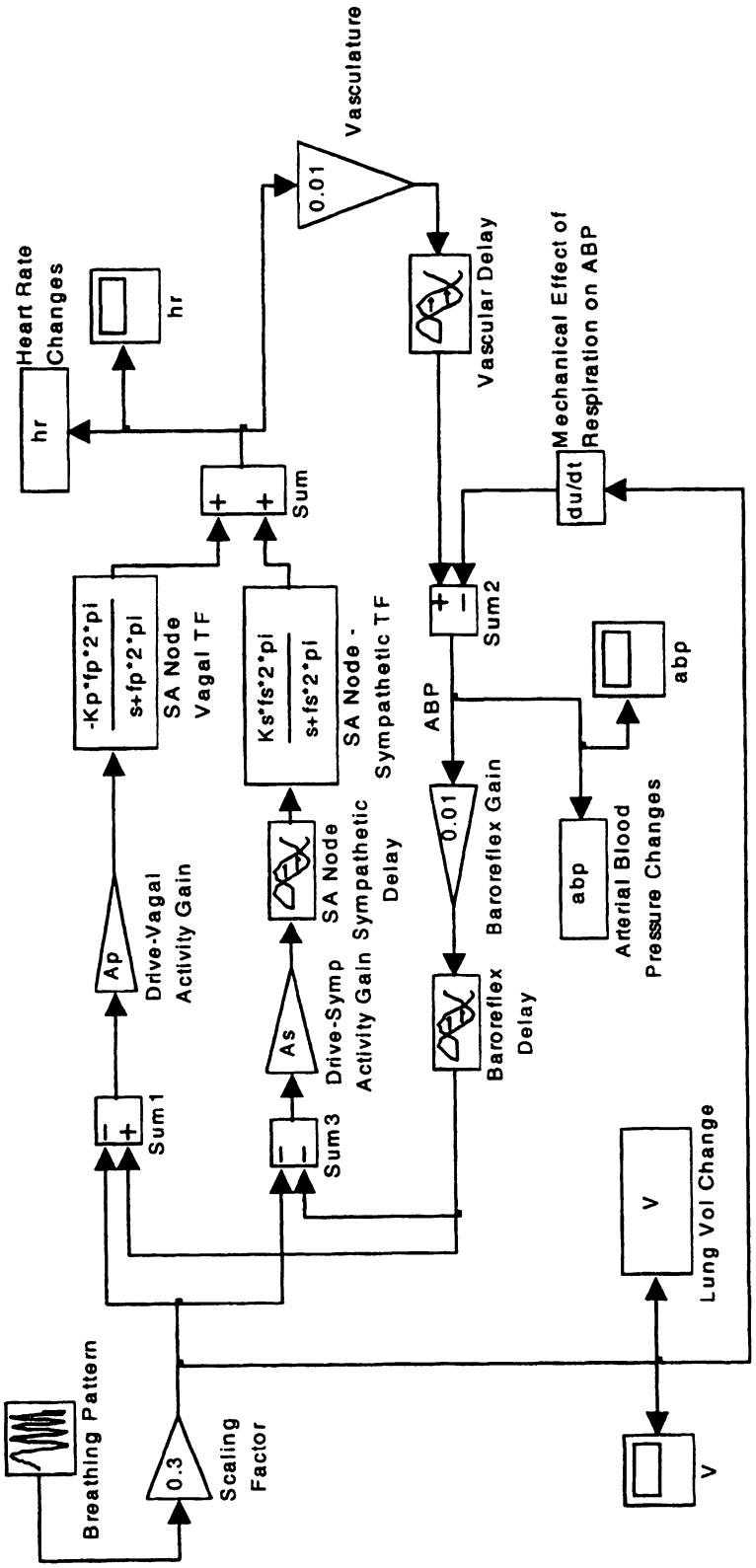

Figure 5.13 SIMULINK model of circulatory control that accounts for the effect of respiration on heart rate and arterial blood pressure.

transduction of abp into baroreceptor output occurs with very rapid dynamics, we assume that the baroreflex can be adequately represented by a static gain (equal to 0.01) in series with a fixed delay of 0.3 s. Finally, the direct mechanical effects of respiration on abp are modeled as a negative differentiator, i.e., inspiration tends to decrease abp while expiration tends to increase it. Thus, the model simulates respiratory sinus arrhythmia by allowing the direct autonomic stimulation of heart rate. As well, the resulting changes in heart rate and the direct mechanical effects of respiration produce fluctuations in abp, which subsequently affect hr via the baroreflexes.

5.4.2 Simulations with the Model

To determine the frequency response of the circulatory control model, we employ a source block that produces a chirp signal. This is a sine wave, the frequency of which increases linearly with time. In our case, we set the parameters of the chirp block such that we start off with a frequency of 0.005 Hz and end with a frequency of 0.5 Hz after a duration of 300 s (simulation time). Since the amplitude of the chirp signal is not adjustable, a gain block of 0.3 is included between the source block and the rest of the model. This limits the peak-to-peak amplitude of the "respiration signal" to 0.6 liter. Before starting the simulation, the m-file "rsa_var.m" has to be executed in order to assign values to the adjustable parameters of the model. The following nominal parameter values represent the normal subject in supine posture: SA node vagal transfer function gain, $K_p = 6$; SA node sympathetic transfer function gain, $K_s = 18$; SA node vagal transfer function cutoff frequency, $f_p = 0.2$ Hz; SA node sympathetic transfer function cutoff frequency, $f_s = 0.015$ Hz. The relative weight factors for the conversion of respiratory drive or baroreflex drive to efferent neural activity are: A_p (for the vagal branch) $= 2.5$ and A_s (for the sympathetic branch) $= 0.4$.

Figure 5.14 displays the results obtained from one simulation run; for the sake of clarity, only 100 s of the simulated "data" are shown. The top panel shows the chirp signal (respiratory input) used to stimulate the model. The corresponding changes in heart rate predicted by the model are displayed in the middle panel. Note that at low frequencies, heart rate fluctuates almost in synchrony with lung volume change; however, at the higher frequencies, it tends to lag respiration. Also, the amplitude of the heart rate signal decreases with increasing frequency, underscoring the low-pass nature of the overall frequency response. The predicted behavior of arterial blood pressure is somewhat different: as frequency increases, the respiratory-induced changes in abp become larger. This results from the growing influence of the direct mechanical effects of breathing on blood pressure as frequency increases.

5.4.3 Frequency Response of the Model

Using the method described in Section 5.3.2, the frequency response of the model can be deduced from the input and simulated output. Instead of inserting the Spectrum Analyzer block, the reader can also save the input (V) and output (hr or abp) variables to the Workspace, and use the following MATLAB code (saved as "rsa_tf.m") to deduce the frequency response:

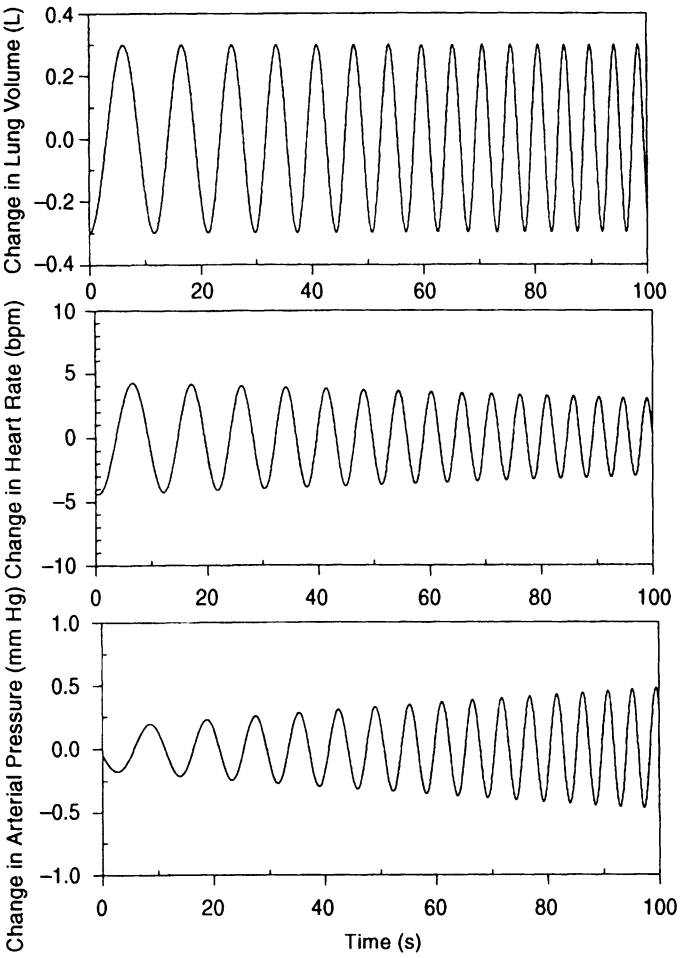

Figure 5.14 Responses in heart rate and arterial blood pressure to a controlled breathing pattern (slow-to-high frequency), as predicted by the SIMULINK model of circulatory control ("normal" conditions).

```
% We assume the sampling interval is 0.1 s so that N = 3000
% for a total simulation time of 300 s
>>freq = [0:1/300:5]';
% compute Power spectrum of V and Cross-spectrum between
% V and hr
>> Pv = psd(V, N, 10);
>> Pvhr = csd(V, hr, N,10);
% compute Frequency Response magnitude and phase
>> Hvhr = Pvhr./Pv;
>> Hvhrmag =abs(Hvhr);
>> Hvhrpha = angle(Hvhr)*180/pi;
```

The chirp signal is useful as an input waveform since it produces a reasonably broad spectrum over the frequency range of interest: 0 to 0.4 Hz. Figure 5.15 displays the magnitude (top

panel) and phase (lower panel) components of the frequency response between respiration and heart rate estimated for the simulated supine normal subject (solid curves). The low-pass nature of the magnitude response is clearly evident; however, the frequency response values toward the low (0 Hz) and high (0.4 Hz) ends of the range displayed cannot be regarded as accurate since most of the spectral power of the chirp input is contained in the frequencies in the middle of this range.

The results of two other simulation cases are also presented in Figure 5.15. The first simulates how the frequency response of the respiratory sinus arrhythmia would change if the "subject" were given a dose of atropine ("+Atropine", dashed curves) that produces complete *parasympathetic blockade*. In addition, the model parameters are also modified to simulate the subject in a standing posture, when the sympathetic influence on heart rate is enhanced. Under such conditions, heart rate control would be modulated predominantly by the sympathetic nervous system. Not surprisingly, the resulting frequency response magnitude curve shows a substantial increase at frequencies below 0.03 Hz and a large decrease at frequencies higher than 0.1 Hz. The phase curve shows a much steeper slope, indicating an

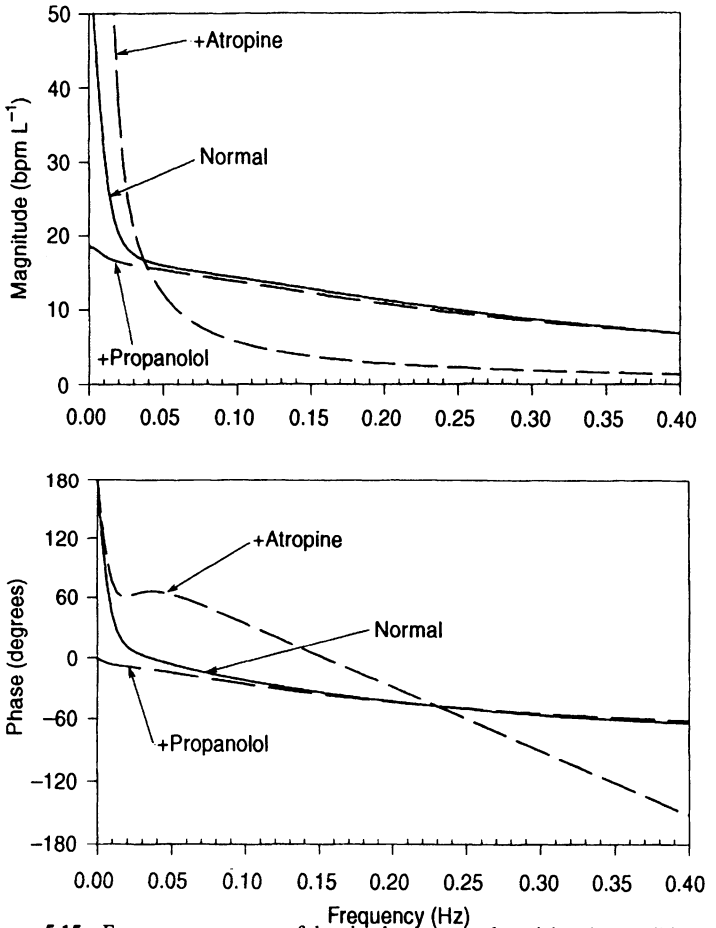

Figure 5.15 Frequency responses of the circulatory control model under conditions that simulate normal heart rate control, complete β-adrenergic blockade ("+Atropine"), and complete parasympathetic blockade ("+Propanolol").

increase in the lags inherent in the system. The values of the model parameters employed here are: $A_p = 0.1$, $K_p = 1$, $f_p = 0.07$ Hz, $A_s = 4.0$, $K_s = 9$ and $f_s = 0.015$ Hz.

In the other simulation case, the "subject" is given a dose of propanolol, which produces *β-adrenergic blockade*. Furthermore, we assume a supine posture, thus making vagal modulation the predominant mode of control. The frequency response curves corresponding to this condition are labeled "+Propanolol". Compared to the control case, there is little change in the frequency response above 0.05 Hz. However, loss of sympathetic modulation leads to a significant decrease in frequency response magnitude and phase at the very low frequencies. Under this "purely vagal" state, the phase difference between respiration and heart rate is relatively small over the 0 to 0.4 Hz range, indicating that the respiratory-induced changes in heart rate occur rapidly. The parameter values used to represent this state are: $A_p = 2.5$, $K_p = 6$, $f_p = 0.2$ Hz, $A_s = 0.1$, $K_s = 1$, $f_s = 0.015$ Hz.

5.5 FREQUENCY RESPONSE OF GLUCOSE–INSULIN REGULATION

In Section 3.6, we examined the model of glucose and insulin regulation proposed by Stolwijk and Hardy but limited the scope of our analysis to the steady state. Here, we present the complete, dynamic version of this model as well as its SIMULINK implementation.

5.5.1 The Model

Employing the same notation as that presented in Section 3.6, Equations (3.40a) and (3.40b), which characterize the mass balance of glucose in the blood plasma, may be extended to incorporate dynamics in the following way:

$$C_G \frac{dx}{dt} = U(t) + Q_L - \lambda x - vxy, \qquad x \leq \theta \tag{5.31a}$$

$$C_G \frac{dx}{dt} = U(t) + Q_L - \lambda x - vxy - \mu(x - \theta), \qquad x > \theta \tag{5.31b}$$

In the above equations, C_G represents the glucose capacitance in the extracellular space and $U(t)$ represents the time-course with which external glucose is infused into the bloodstream, as part of the "glucose tolerance test." Basically, Equations (5.31a) and (5.31b) state that the net difference between the rate at which glucose is added to the blood and the rate at which it is eliminated equals the rate at which the glucose concentration, x, will increase (or decrease). It is important to note that the cross-product term between x and y, the insulin concentration, makes the above equations nonlinear (or strictly speaking, bilinear). The corresponding dynamic mass balance for insulin is simply a straightforward extension of Equations (3.43a) and (3.43b):

$$C_I \frac{dy}{dt} = -\alpha y, \qquad x \leq \phi \tag{5.32a}$$

$$C_I \frac{dy}{dt} = -\alpha y + \beta(x - \phi), \qquad x > \phi \tag{5.32b}$$

where C_I is the insulin capacitance of the extracellular space.

The SIMULINK implementation of this model (filename "`glucose.mdl`") is displayed in Figure 5.16b. The top half of the interconnected block structures represents Equations (5.31a) and (5.31b), characterizing the dynamics of blood glucose build-up and elimination, while the bottom half models insulin dynamics, as described by Equations

(5.32a) and (5.32b). Saturation blocks are employed to function as thresholding operators, with the lower limit set equal to zero and the upper limit set equal to a very large number (so that there is effectively no saturation at the high end). One of these saturation blocks allows for the disappearance of the last term in Equation (5.31b) when $x \leq \theta$, where θ is the threshold concentration below which all glucose is reabsorbed in the kidneys, which results in no glucose loss in urine. The other saturation block in the insulin portion of the model allows for the disappearance of the last term in Equation (5.32b) when $x \leq \phi$, where ϕ is the threshold glucose concentration for insulin secretion.

The glucose–insulin regulation model is encapsulated into a `Subsystem` block, which is shown in relation to the source and sink blocks in Figure 5.16a. The `Subsystem` block is created by dragging its icon from the `Connections` block library to the model window. By double-clicking on the `Subsystem` block, a subsystem window will appear and the user can proceed to create the model in question within this window. `Inport` blocks are used for all signals entering the subsystem while `Outport` blocks form the terminal points for all signals leaving the subsystem.

5.5.2 Simulations with the Model

Glucose infusion into the model is simulated through the use of a `pulse generator` block, which produces a rectangular wave. The period of the output waveform is set equal to the simulation time of 5 hours, with time step being 0.01 hour. The duty cycle is set to 5% so that glucose infusion occurs over a duration of 0.25 hour or 15 minutes, starting at $t = 0.5$ hours. The glucose infusion rate (amplitude of the rectangular wave) is set equal to $100\,000\,\text{mg}\,\text{h}^{-1}$.

Examples of two simulation runs are displayed in Figure 5.17. The input waveform is shown in the top panel of this figure. The resulting time-courses in glucose concentration and insulin concentration are shown in the middle and lower panels, respectively. Two classes of subjects are examined here: the normal adult (solid curves) and the Type-2 diabetic (dashed curves). Note that in the diabetic, the steady-state levels for glucose and insulin are both higher than corresponding levels in the normal, which confirms what we found by a graphical method of solution in Section 3.6. As well, in the diabetic, the decay of glucose and insulin concentrations toward steady-state levels following the infusion is noticeably slower compared to the normal subject. Furthermore, the glucose time-course does not show the slight undershoot exhibited by the corresponding time-course in the normal.

5.5.3 Frequency Responses of the Model

Using the method outlined in Section 5.3.2 (see MATLAB m-file "`gireg.m`"), estimates of the frequency responses of this model are deduced and shown in Figure 5.18. The top panel displays the frequency response magnitude curves (H_{ux}) relating the glucose infusion to resulting glucose concentration for both normal and Type-2 diabetic. The slower response of the diabetic is reflected in the higher values for the frequency response magnitude at frequencies below $0.4\,\text{cycles}\,\text{h}^{-1}$. The frequency response magnitude curve for insulin (H_{uy}) shows a very similar shape (middle panel of Figure 5.18). Finally, we also display the frequency response relating glucose concentration as input to insulin concentration as output

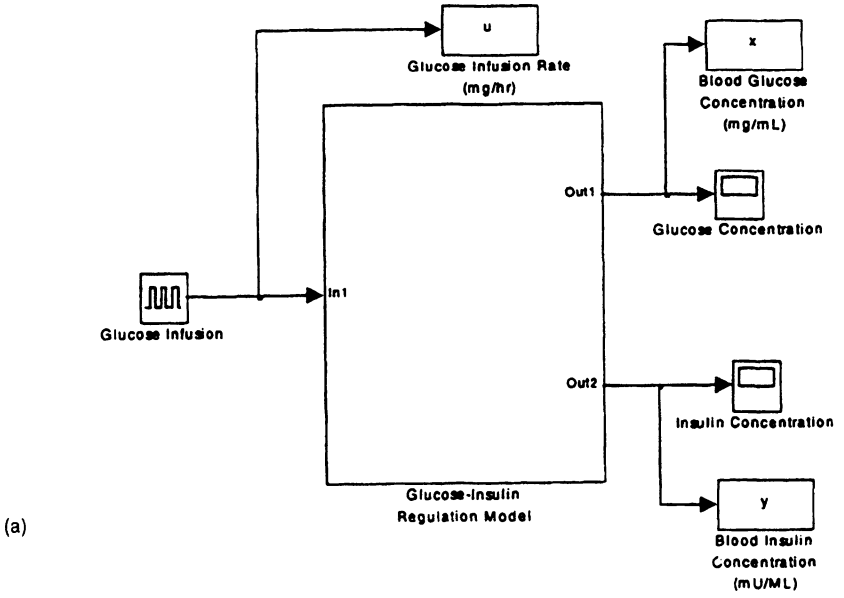

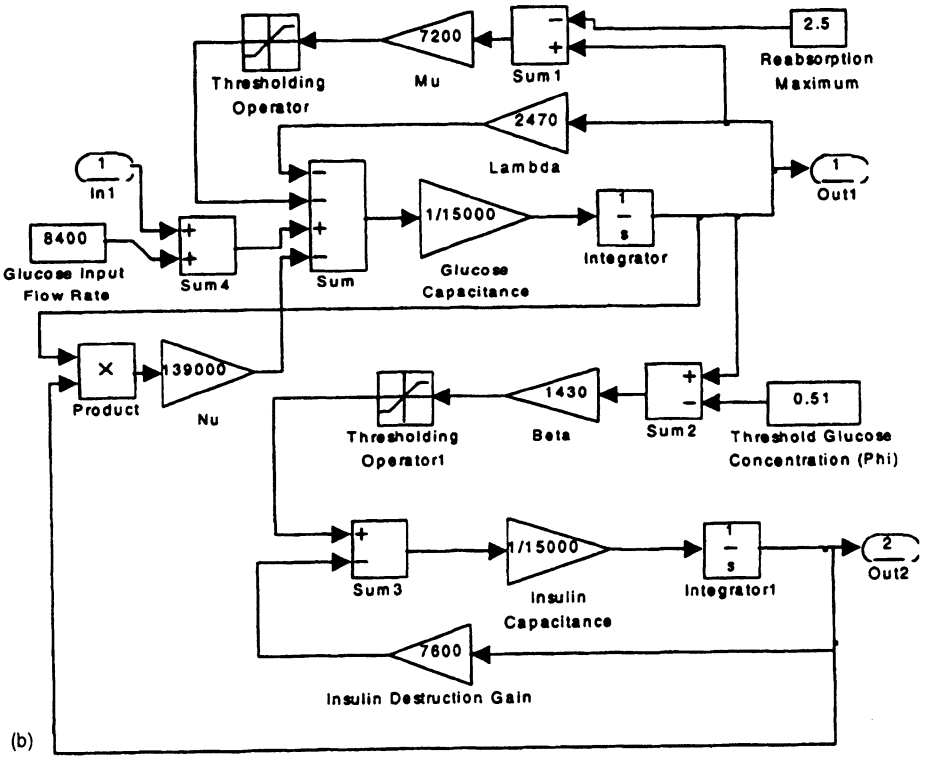

Figure 5.16 SIMULINK model of blood glucose–insulin regulation. (a) The input to and outputs from the model. (b) Details of the dynamic structure.

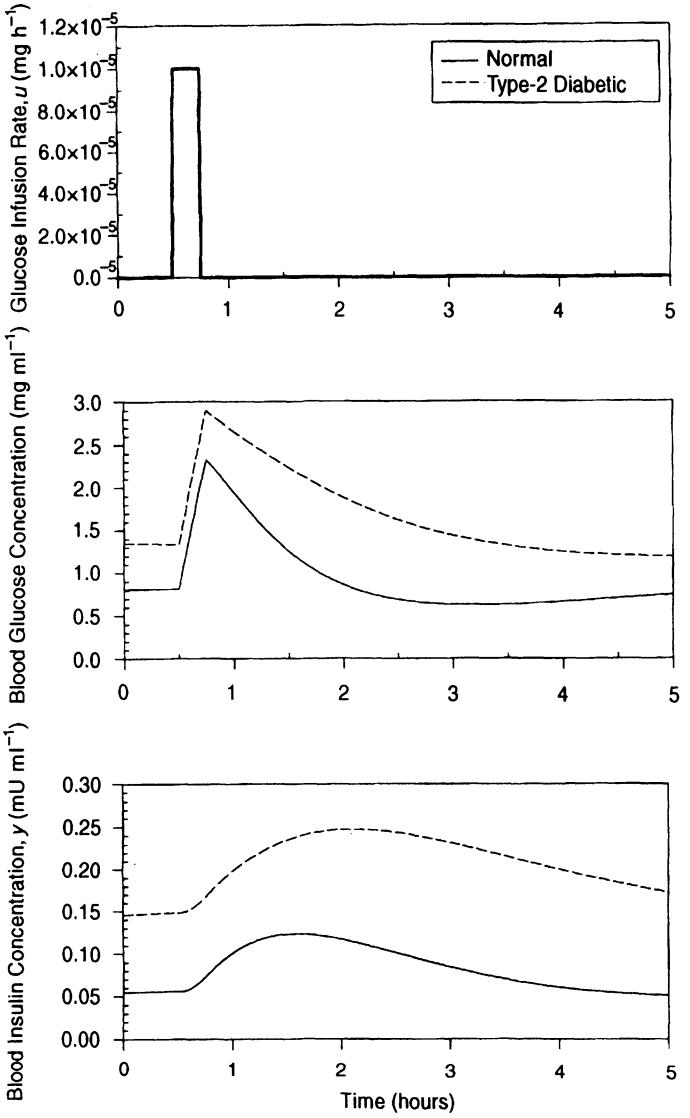

Figure 5.17 Response of the glucose–insulin regulation model to a rapid (15 min) infusion of 25 g of glucose in a simulated normal human (solid lines) and a Type-2 diabetic (dashed lines).

(H_{xy}). In this case, the transfer magnitude for the diabetic is higher than the normal over a much wider range of frequencies (0 to 1 cycle h^{-1}).

An important point to note in this example is that there are a number of nonlinearities embedded in the model: the thresholds θ and ϕ, as well as the multiplicative interaction between x and y. These are clearly exhibited in the steady-state curves representing glucose–insulin regulation in Figure 3.13. Therefore, strictly speaking, the application of frequency response analysis, a linear technique, is not valid. On the other hand, it is also clear, from the graphs presented in Figure 3.13, that the degree of nonlinearity is not so high as to preclude replacing segments of the hyperbolic relationship with piecewise linear approximations. Thus, assuming that the fluctuations in x and y are reasonably limited in range, particularly under physiological conditions, frequency response analysis remains useful in providing some insight into the dynamic behavior of this system.

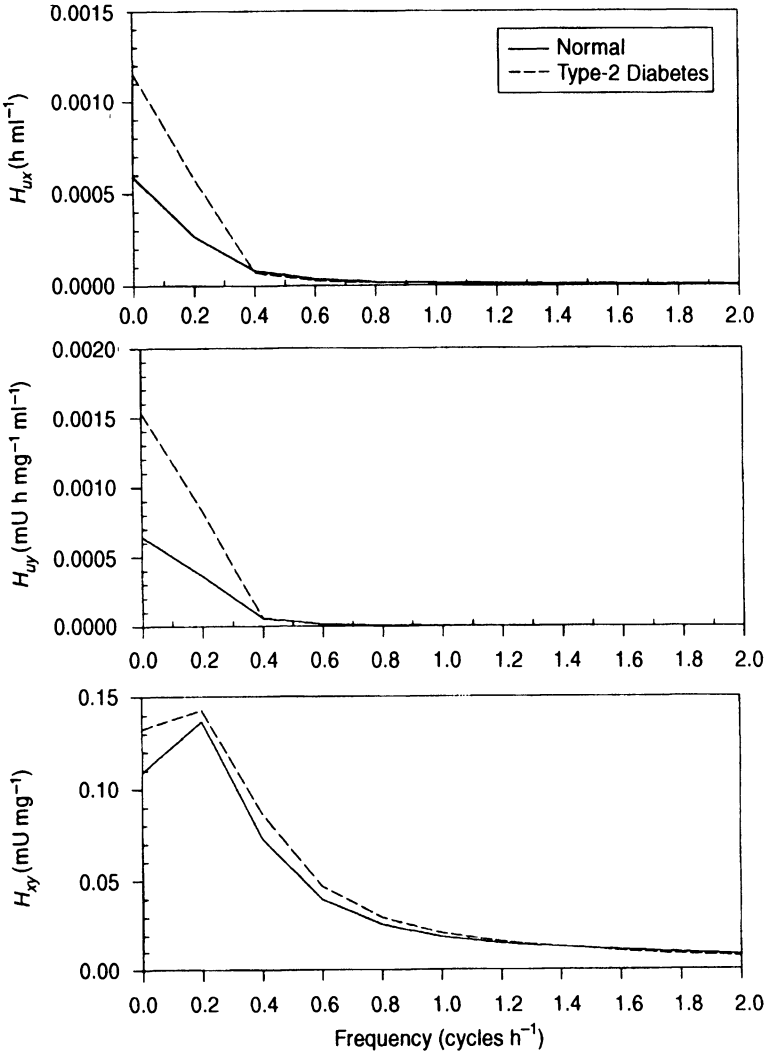

Figure 5.18 Frequency responses of glucose–insulin regulation model in conditions simulating a typical normal human (solid lines) and a Type-2 diabetic (dashed lines).

BIBLIOGRAPHY

Dorf, R.C., and R.H. Bishop. *Modern Control Systems*, 7th ed. Addison-Wesley, Reading, MA, 1995.

Kuo, B.C. *Automatic Control Systems*, 4th ed. Prentice-Hall, Englewood Cliffs, NJ, 1994.

Milhorn, H.T. *The Application of Control Theory to Physiological Systems*. W.B. Saunders, Philadelphia, 1966.

Milsum, J.H. *Biological Control Systems Analysis*. McGraw-Hill, New York, 1966.

Morris, N.M. *Control Engineering*, 4th ed. McGraw-Hill (UK), London, 1991.

Saul, J.P., R.D. Berger, P. Albrecht, S.P. Stein, M.H. Chen, and R.J. Cohen. Transfer function analysis of the circulation: unique insights into cardiovascular regulation. *Am. J. Physiol.* **261** (*Heart Circ. Physiol.* **30**): H1231–H1245, 1991.

Soechting, J.F., P.A. Stewart, R.H. Hawley, P.R. Paslay, and J. Duffy. Evaluation of neuromuscular parameters describing human reflex motion. *Trans. ASME, Series G* **93**: 221–226, 1971.

Stolwijk, J.E., and J.D. Hardy. Regulation and control in physiology. In: *Medical Physiology*, 13th ed. (edited by V.B. Mountcastle). C.V. Mosby, St. Louis, 1974; pp. 1343–1358.

Strum, R.D., and D.E. Kirk. *Contemporary Linear Systems using MATLAB*. PWS Publishing Co., Boston, MA, 1994.

PROBLEMS

P5.1. Consider the simplified model of eye-movement control displayed in Figure P4.1. Assuming that $G/J = 14{,}400\,\text{rad}^2\,\text{s}^{-2}$, $B/J = 24\,\text{rad}\,\text{s}^{-1}$ and $k_v = 0.01$, compute the frequency response for this model. Display the magnitude and phase components of the frequency response in the form of:
(a) linear-scale frequency response plots (e.g., Figures 5.2 and 5.3);
(b) Bode plots;
(c) Nichols charts;
(d) Nyquist plots.

P5.2. In the eye-movement control model considered above, determine how the frequency response of the model would change if:
(a) there is no velocity feedback ($k_v = 0$);
(b) the velocity feedback gain is negative ($k_v < 0$).

Employ the parameter values given in Problem P5.1. Compare the control case ($k_v = 0.01$) to cases (a) and (b) using linear-scale frequency response plots.

P5.3. Compute and plot the frequency responses of the system shown in Figure P4.2 when:
(a) the feedback loop is open; and
(b) the feedback loop is closed.

In both cases, assume the time delay, T, to be 1 second.

P5.4. Determine the frequency responses of the ventilatory control model shown in Figure P4.3, assuming (a) $\alpha = 0$ (no rate sensitivity); (b) $\alpha = \frac{1}{2}$ (lag–lead feedback); and (c) $\alpha = 2$ (lead–lag feedback).

P5.5. Derive a closed-form expression for the frequency response of the circulatory control model shown in Figure 5.13, with respiration as the input and heart rate as the output. Using the parameter values given in the SIMULINK implementation of the model ("`rsa.mdl`") and Section 5.4.3, deduce and plot the frequency responses of this model for the three cases shown in Figure 5.15: (a) normal supine subject; (b) following atropine administration; and (c) following propanolol infusion. Compare these plots with those presented in Figure 5.15.

P5.6. The model of Figure 5.13 can be used to investigate the dynamics of blood pressure regulation by the baroreflexes in the following way. In the SIMULINK model, "`rsa.mdl`," remove the respiratory input from the model and add an external source that imposes a random excitation directly on arterial blood pressure. This can be achieved experimentally in approximate fashion by imposing positive and negative pressure changes on the neck, thereby changing carotid sinus pressure. Assuming the applied pressure time-course to be the input and the resulting heart rate changes to be the output, use the method outlined in Section 5.3.2 to deduce the frequency response of the closed-loop baroreflex control system.

P5.7. Derive an expression for the closed-loop frequency response of the neuromuscular reflex model displayed in Figure 4.11, assuming the external moment, M_x, to be the

input and angular displacement of the forearm, θ, to be the output. Using the parameter values given in Section 4.6.2, display the magnitude and phase plots of the frequency response.

P5.8. Using the SIMULINK implementation of the neuromuscular reflex model ("`nmrflx.mdl`"), displayed in Figure 4.12, estimate the frequency response of the closed-loop system by using the method discussed in Section 5.3.2. Employ a random noise source as the driving input, M_x. Check your results against the magnitude and phase plots of frequency response deduced analytically in Problem P5.7.